Thomson spectrometer-microchannel plate assembly calibration for MeV-range positive and negative ions, and neutral atoms

AIP | Review of Scientific Instruments

Thomson spectrometer–microchannel plate assembly calibration for MeV-range positive and negative ions, and neutral atoms

R. Prasad, F. Abicht, M. Borghesi, J. Braenzel, P. V. Nickles et al.

Citation: Rev. Sci. Instrum. **84**, 053302 (2013); doi: 10.1063/1.4803670
View online: http://dx.doi.org/10.1063/1.4803670
View Table of Contents: http://rsi.aip.org/resource/1/RSINAK/v84/i5
Published by the AIP Publishing LLC.

Thomson spectrometer–microchannel plate assembly calibration for MeV-range positive and negative ions, and neutral atoms

R. Prasad,[1] F. Abicht,[2] M. Borghesi,[1,3] J. Braenzel,[2] P. V. Nickles,[4] G. Priebe,[2] M. Schnürer,[2] and S. Ter-Avetisyan[1,3]
[1]*Centre for Plasma Physics, School of Mathematics and Physics, The Queen's University of Belfast, Belfast BT7 1NN, United Kingdom*
[2]*Max Born Institute for Nonlinear Optics and Short Pulse Spectroscopy, 12489 Berlin, Germany*
[3]*ELI-Beamlines Project, Institute of Physics of the ASCR, Na Slovance 2, 18221 Prague, Czech Republic*
[4]*WCU Department of Nanobio Materials and Electronics, GIST, Gwangju 500-712, South Korea*

(Received 4 December 2012; accepted 18 April 2013; published online 9 May 2013)

We report on the absolute calibration of a microchannel plate (MCP) detector, used in conjunction with a Thomson parabola spectrometer. The calibration delivers the relation between a registered count numbers in the CCD camera (on which the MCP phosphor screen is imaged) and the number of ions incident on MCP. The particle response of the MCP is evaluated for positive, negative, and neutral particles at energies below 1 MeV. As the response of MCP depends on the energy and the species of the ions, the calibration is fundamental for the correct interpretation of the experimental results. The calibration method and arrangement exploits the unique emission symmetry of a specific source of fast ions and atoms driven by a high power laser. [http://dx.doi.org/10.1063/1.4803670]

INTRODUCTION

Laser-driven acceleration of ions is a rapidly growing field of research. State-of-the-art laser systems allow to accelerate bunches of positive ions with unique properties: high brightness, kilo-Ampere current,[1] ultralow emittance,[2] and ∼ps burst duration[3,4] which leads to bright prospects for numerous innovative applications.[5] Recently a novel spray target[6] was introduced as an ion source displaying specific features such as a copious emission of negative oxygen ions, observed together with positive oxygen ions and a significant number of neutral atoms.

Negative ions are used in many processing applications[7,8] and in accelerator technology,[9,10] including injectors for heating Tokamak plasmas.[11,12] A quantitative analysis of these particles is very important as their number, momentum, and temporal profile are closely related to the dynamics of the acceleration processes, and an enhanced understanding of these processes may allow controlling the beam properties as required by many foreseen applications.

Numerous detectors have been used in the past decades to record high-energy charged particles. These include solid state nuclear track detectors such as CR-39,[13] nuclear emulsions, radiochromic films (RCFs),[14] image/phosphor plates,[15] scintillators, Cherenkov detectors, Faraday cups, or MCPs. As an online ion detector, MCPs coupled to the phosphor screen have been successfully used as detectors in Thomson[16] mass-spectrometers, to analyse laser accelerated, multi-component charged particle beams, providing the distribution of energetic particles as a function of their momentum and mass-to-charge ratio.

Recently the response of a MCP detector, assembled in a Thomson spectrometer to investigate laser accelerated charged particles, was calibrated[17] by measuring the ratio between the count numbers in the charge-coupled device (CCD) image of the phosphor screen and the number of incidence ions. The particle response of the whole detection system was evaluated for protons from 0.8 MeV up to 3 MeV and carbon ions from 3 MeV up to 16 MeV. From the results[17] one can see that the MCP response depends on the energy and the species of the particles, showing that the calibration of the detector is fundamental for a correct interpretation of the experimental results, especially for different charged ions species: positive-, negative-, or neutral particles.

This paper describes the calibration of the response of a Thomson–MCP assembly to the impact of protons and positive, negative, and neutral oxygen atoms. The calibration method and arrangement exploits the unique emission symmetry of a specific source of fast ions and atoms driven by a high power laser. We will discuss the method employed, and the relevant data analysis for this *in situ* calibration.

SETUP AND CALIBRATION METHOD

A water spray target consisting of 150 ± 10 nm liquid droplets was irradiated by 40 fs, 1 J Ti:Sapphire laser pulses at the High-Field-Laser-Application Laboratory of the Max-Born-Institute. With a f/2.5 off-axis parabolic mirror an intensity of $\sim 5 \times 10^{19}$ W/cm^2 was achieved. The ion spectra were measured in both axisymmetric transverse directions (±90° with respect to the laser axis) simultaneously in a single laser shot (Fig. 1) using two identical Thomson parabola spectrometers, both including a MCP detector coupled to a phosphor screen. The image of the phosphor screen was taken with a cooled 12 bit Chroma CCD camera. A symmetric ion emission was observed in both lateral directions when the laser pulse was focused in the centre of the spray. This feature has enabled us to measure the absolute number of the emitted particles using CR-39 detector on one of these two lines

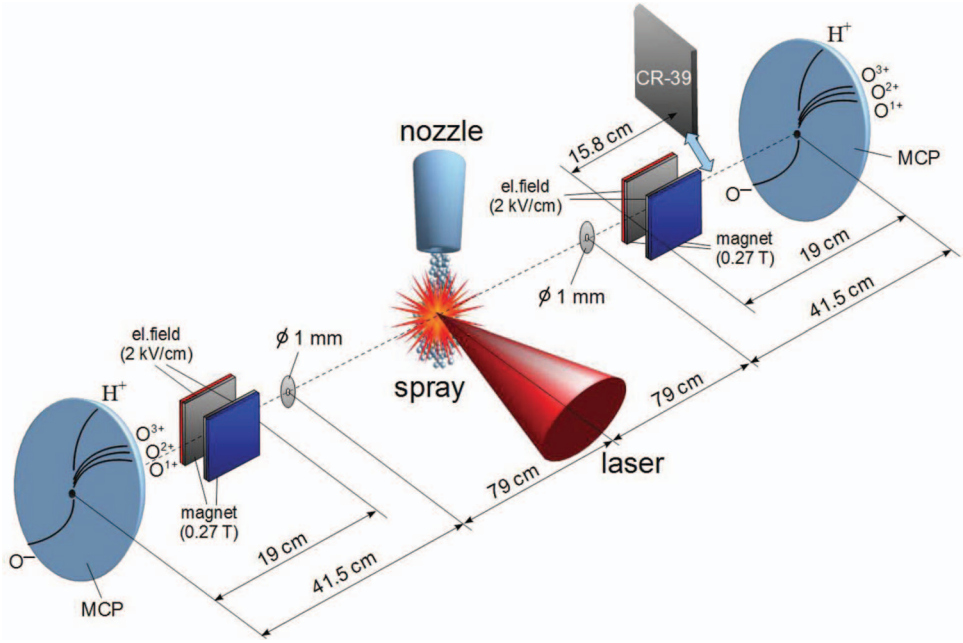

FIG. 1. Schematic of measuring the response of MCP to positive, negative, and neutral oxygen from spray target.

(e.g., −90° side spectrometer) and to compare it with the count number on the CCD image of the phosphor screen of the MCP detector obtained on the other line (+90° side spectrometer).

In order to avoid artefacts caused by the different angles of incidence onto the MCP channels of the ions dispersed along the spectra, the MCP is installed in such a way that the bias angle of the channels is in a horizontal plane, parallel to the electric and magnetic fields of the spectrometer. In this case the angle of incidence of the spectrally dispersed ions stays approximately constant for all energies along the MCP surface. A total number of 15 shots were accumulated on the −90° spectrometer using a CR-39 detector whereas the spectrum for each corresponding shot was recorded on the +90° spectrometer using the MCP detector.

The CR-39 plate was etched in 6*N* NaOH solution to retrieve the incident particle number. Since the stopping power of oxygen ions with energy up to hundreds of keV is low, we have etched the CR-39 in 10 min steps for an overall duration of 30 min. The resulting pits were counted using an optical microscope. The spectra were analysed using a routine in MATLAB to identify the ion species and their energies. Protons, O^+, O^{2+}, and O^- ions are detected on both the CR-39 and MCP detectors. The number of counts measured in the ion tracks (or spectra) imaged on the CCD was compared with the number of ions obtained from the etched CR-39 detector for the same ion species.

A lower energy cutoff on the MCP detector, 16 keV for O^+ and 160 keV for protons, appears due to the finite size of the detector and the chosen geometry of the spectrometer. On the CR-39 detector it was hard to recognize oxygen ions with energies below 79 keV due to their low stopping range, and tracks caused by protons were visible down to energies of 40 keV.

Ion acceleration from the spray target is understood in a scenario based on a combined thermal expansion-Coulomb explosion (CE) hybrid model of a single droplet.[18] However, during the propagation of accelerated ions through the spray, their charge state and spectral distribution are strongly modified due to the interaction with the cold particle cloud (the spray). In these interactions the energetic ions can capture or lose electrons and therefore can change their charge state becoming negative or neutral,[6] while their kinetic energy is conserved.

In contrast to the negative and positive ions, which are deflected in the spectrometer in opposite directions, neutrals are detected at the so called "zero-point" of the spectrometer, where undeflected particles or photons (X-rays, γ-rays, or neutral atoms) emitted from the laser plasma interaction region impact on the MCP. Since CR-39 is insensitive to photons, the pits observed at the "zero-point" on the CR-39 detector (see Fig. 2) result from energetic neutral atoms. In Fig. 2(a), pits formed by oxygen ions in the O^+ spectral track are shown, whereas pits from the proton track are shown in Fig. 2(c). In the central image, Fig. 2(b), pits at the "zero-point" are shown. It is easy to see that the "zero-point" consists of both hydrogen and oxygen atoms. The hydrogen pit size on CR-39 was almost half than for the pits made by oxygen ions.

The shot-to-shot fluctuations in the ion spectra were relatively small. Fluctuations in ion number were of the order of 10% and could be attributed to shot-to-shot variations of the laser pulse parameters, beam pointing and spray performance. The maximum energies of ions were even more stable, probably also due to the absence of a clear cutoff at high energies. Overall stable emission from the spray is related to the collisional nature of emission, where all the processes are smoothed out. However, it should be noticed that fluctuations

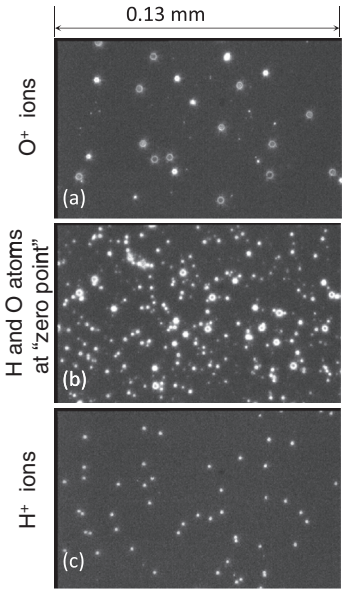

FIG. 2. Picture of ion pits detected on CR-39. Pits of (a) oxygen and (c) hydrogen ions along their spectral tracks. Pits in (b) is zoomed picture of "zero point" showing similarity with the (a) oxygen and (c) hydrogen ions pits.

are present only in the ions absolute values and even so fluctuations would not play a role in the relation between ion signal from different detectors taken in the same shot and affect the calibration results.

MCP RESPONSE TO O^+ AND O^{2+}

The number of particles on CR-39 in a given energy interval along a track is correlated with the integrated counts on the CCD referring to the same energy interval and track. The correlation between integrated counts on MCP and particle number on CR-39 in the corresponding energy interval is shown in Fig. 3(a).

Since the tracks of O^+ and O^{2+} ions on the CR-39 plate were merged together at higher energies (>240 keV) and the sizes of the pits for O^+ and O^{2+} were found to be the same, the MCP response to these two ions has been taken to be the same. For this reason the counts of O^+ and O^{2+} ions on CR-39 plate were integrated along the tracks if it were single particle pits, as well as those ion tracks on MCP image. The response of MCP to O^+ and O^{2+} ions has been calculated by dividing the integrated counts for a certain energy interval over the MCP image with the total particle numbers observed on CR-39 in the corresponding energy interval. The response of MCP over the energy range from 0.43 MeV to 3 MeV is shown in Fig. 3(b). It is obvious, that the MCP response to O^+ and O^{2+} ions is almost constant over the calculated energy range.

MCP RESPONSE TO O^-

The response of MCP to O^- ions has been calculated, in a similar way, by dividing the counts for a certain energy interval of the MCP image by the total particle numbers on the CR-39 plate in the same energy interval. A difference is that in this case, the particle number was relatively lower than the positive oxygen ions and the energy range comparatively smaller, which result in a larger counting error (about 10%) at low energies (~0.08 MeV). Nevertheless, at higher energies (0.4 MeV), where the particle pits were clearly countable, the response is close to the response for O^+ and O^{2+}. The average response near 0.4 MeV is indicated by squares in Fig. 3(b).

MCP RESPONSE TO H^+

In the same shots, protons up to 1 MeV were also accelerated. The calibration obtained with these protons extends our previous calibration of the MCP detector response to protons (see Ref. 17) to a lower energy range (0.16–0.5 MeV). The correlation between the integrated counts on MCP and the total number of particles on CR-39 is shown in Fig. 4(a) and the MCP response in Fig. 4(b). The response could be obtained only in the energy range of 0.16–0.65 MeV, although the maximum cut-off energy was about 1 MeV. This is due to the fact that above 0.65 MeV energy pits on CR-39 were getting smaller and the error in particle counting was

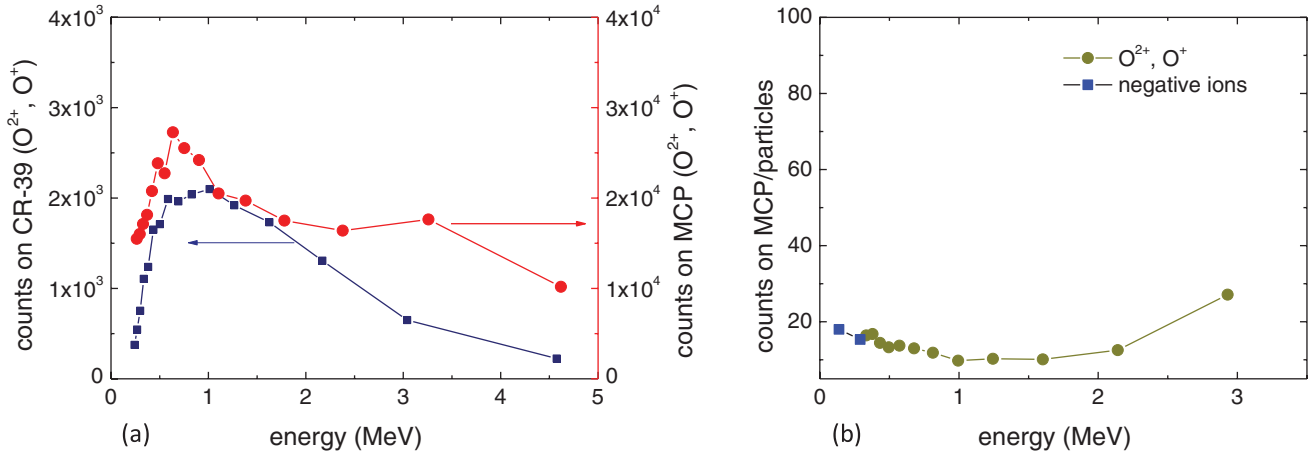

FIG. 3. Calibration of MCP for O^{2+}, O^+ and O^- ions. (a) Correlation of counts on MCP to the particles counted on CR-39 for O^{2+} and O^+ ions together is shown. (b) Response (i.e., counts/particle) of MCP is shown for O^{2+}, O^+ and O^- ions. The blue square points show the average response of MCP to the O^-.

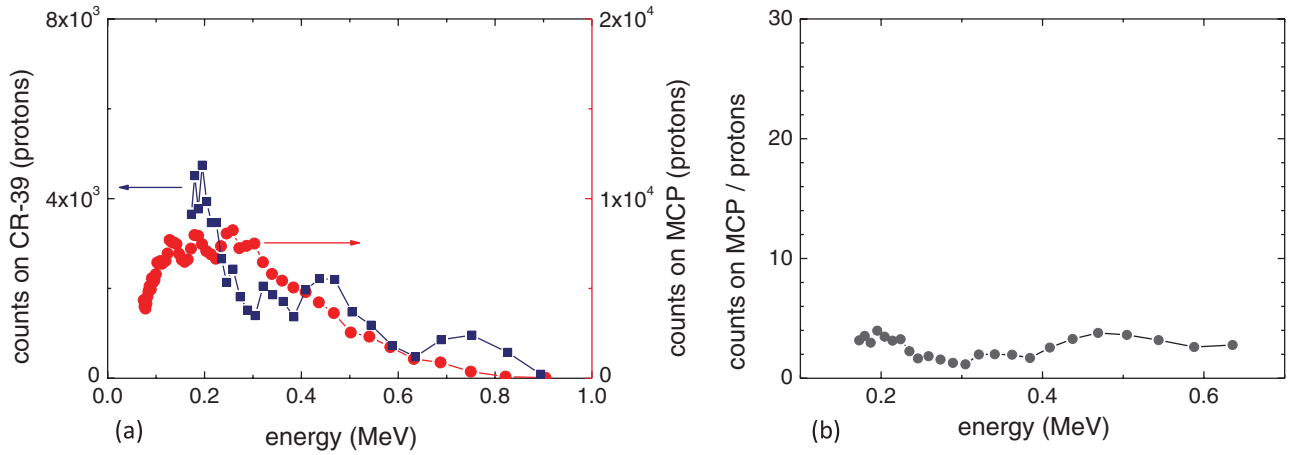

FIG. 4. Calibration of MCP for H^+. (a) The correlation of counts on MCP to the particles counted on CR-39 is shown. (b) Response (i.e., counts/particle) of MCP is shown for H^+.

becoming higher and therefore we restrict our calibration up to 0.65 MeV energy where counting error still below 15%.

MCP RESPONSE TO NEUTRAL ATOMS

As it was shown in Fig. 2, the "zero-point" consists of both hydrogen and oxygen atoms and since the pits are clearly distinguishable, with the hydrogen pit size almost half of the oxygen pit size, it was possible to count the total number of hydrogen and oxygen separately. For the calibration of MCP response to neutral particles several factors have to be taken into account.

First, the MCP image of the "zero-point" is much broader than the simple geometrical projection of the ion source as it is measured on CR-39 plate. This is because the MCP is sensitive to soft X-rays up to ~120 nm wavelengths (for longer wavelengths the detection efficiency becomes less than 1%) and therefore the measured "zero-point" signal comprises the emitted X-ray also. Early measurements have shown that the spatial distribution of the X-ray source is different for different wavelengths (see Fig. 5 in Ref. 19). Shorter wavelengths have the smallest source size, increasing at longer wavelengths. The ions are accelerated from a much hotter region of the plasma, which can be even smaller than the smallest x-ray source size.[19]

In Fig. 5, the distribution of counts across the "zero point" is shown. The "zero point" is the overlap of two distinct Gaussian distributions, one due to the neutrals (narrow distribution), and the other due to the x-rays (we will refer to this as *background* signal). The Gaussian fit of the signal from neutrals has a peak value which is twice the *background* peak and the width (FWHM) is almost half of the background distribution width. At the zero point on the MCP, both hydrogen and oxygen atoms were accumulated and careful analysis was required for calculating the response of hydrogen and oxygen atoms separately.

Second, since the physical mechanism of formation of negative and neutral atoms is the same,[6] they should appear with similar energies. In the spectrometers, charged particles are detected with a low energy cutoff due to the chosen geometry of the spectrometer and the finite size of the detector, whereas for the neutral particles at the "zero-point" there is no such restriction. The "zero-point" on CR-39 contains neutral oxygen and hydrogen atoms (Fig. 2). On the MCP we are detecting negative oxygen, but no negative hydrogen. The spectrometer can measure negative hydrogen with energies above 160 keV, meaning that all the neutral hydrogens which were detected on CR-39 must have energy below 160 keV.

Additionally, we could recognise the pits of negative oxygen ions on CR-39 only above 79 keV (low cut-off energy of the spectrometer for oxygen ions was 16 keV) while lower energies were clearly detectable on MCP. This is due to very small stopping range of oxygen ions in CR-39 at these energies: for 79 keV ions the stopping range is ~2.4 μm which were etched away already within the first 5 min of the etching steps we performed. Therefore, on the basis of the same physical mechanism of formation of negative and neutrals atoms discussed above,[6] one can assume that the neutral oxygen atoms with energies below 79 keV exist and would be detected on MCP. On this basis, one would expect neutral oxygen atoms with energies below 79 keV on MCP image but

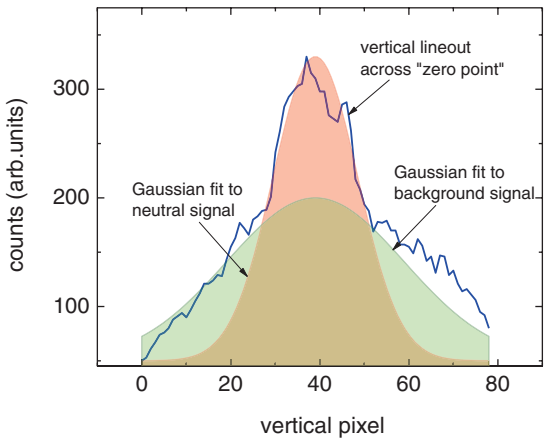

FIG. 5. Distribution of a signal at the "zero point" on MCP. Two distinct different Gaussian functions are necessary to fit the data: one is a signal due to the x-ray, and another due to the energetic neutral particles.

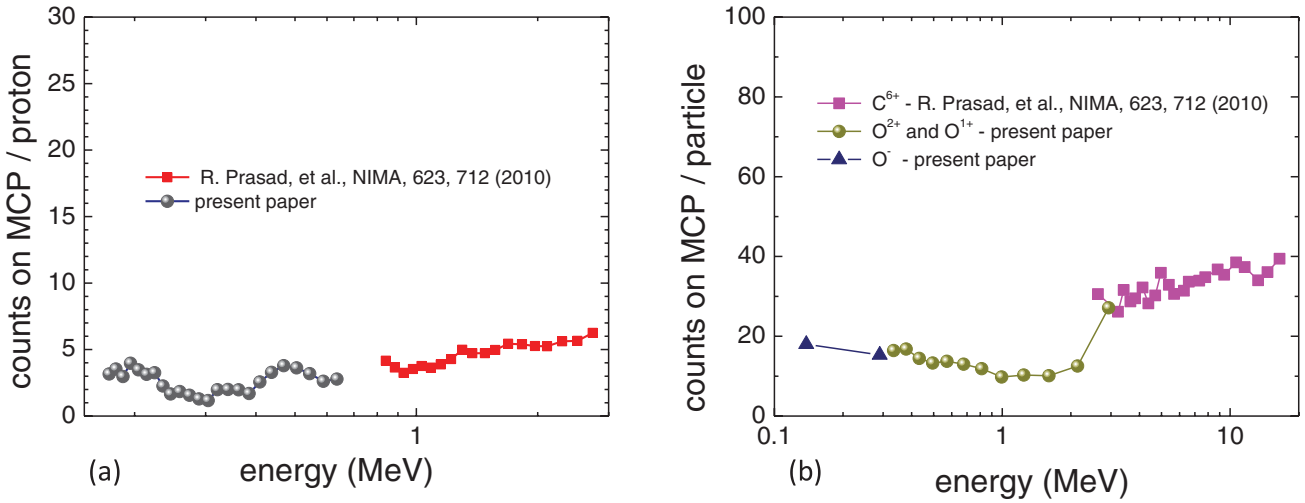

FIG. 6. Comparison of calibration data from Ref. 17 and data presented in this paper.

not on the CR-39 plate, and this has to be considered when interpreting the calibration data.

For hydrogen atoms such consideration is not necessary as at the lower energy cutoff on CR-39 (~40 keV), the pits were still clearly countable. Thus no correction is needed in the case of hydrogen atoms.

In the evaluation of the MCP response to oxygen atoms an important question arises: how many oxygen neutrals have an energy below 79 keV, which are not recorded on the CR-39 plate. In principle, there are two possible ways to evaluate this number. As described in Ref. 6, the main channel for the formation of O^- is mainly via sequential electron capture processes, starting from O^+ and then via O. From the MCP image one can extract the numbers of O^- and O^+ ion. However, the detected O^+ on the MCP result from different reactions, which take place during the propagation of ions through the spray, e.g., $O^{2+} \rightarrow O^+$, $O \rightarrow O^+$. So, the actual number of O^+, which could be held responsible for the formation of the O^-, is difficult to estimate, and the number of O^+ is therefore not useful for the estimation of the neutrals.

On the other hand, one can use O^-, as there the channel for the formation of O^- is mainly via O, while the other reactions contributing to O^- have lower probability. Therefore, a relation between the numbers of O and O^- can be established.

Let us denote the numbers of O^- above 79 keV on MCP by $N^{O^-}_{MCP}(> 79\,\text{keV})$, which can be retrieved from Fig. 3(b), and the number of O above 79 keV on CR-39 by N^{O}_{cr39} $(>79\,\text{keV})$. The ratio of these two quantities can be expressed by α as

$$\alpha = \frac{N^{O}_{cr39}(>79\,\text{keV})}{N^{O^-}_{MCP}(>79\,\text{keV})}$$

and has an value of $\alpha = 1.25$ calculated from our data.

With the same notation we denote the number of O below 79 keV on CR-39 by $N^{O}_{cr39}(<79\,\text{keV})$ and the number of O^- below 79 keV on MCP by $N^{O^-}_{MCP}(<79\,\text{keV})$. Here we know the quantity $N^{O^-}_{MCP}(<79\,\text{keV})$ and α. The quantity $N^{O}_{cr39}(<79\,\text{keV})$ is then calculated as

$$N^{O}_{cr39}(<79\,\text{keV}) = \alpha \times N^{O^-}_{MCP}(<79\,\text{keV})$$

and results in $N^{O^-}_{MCP}(<79\,\text{keV}) = 12681$, hence $N^{O}_{cr39}(<79\,\text{keV}) = 15954$. Therefore, the total number of O on CR-39 in the full/complete energy range is 19 492 (3538 (above 79 keV) +15 954 (below 79 keV)) and the total number of hydrogen is, respectively, ~37 376 on CR-39.

It has to be mentioned that, on the MCP, the area, over which the neutral signal was sampled, was chosen to be exactly the same, as the transverse width of the O^+ tracks (which is defined by the 1 mm pinhole), A background subtraction is carried out by estimating the background in the immediate vicinity of the zero point. After extracting the neutral signal in each shot, the counts for all 15 accumulated shots were added.

Similarly, the same area has been chosen within the "zero point" on CR-39 and the total number of hydrogen atoms has been counted. This count number was related to the counts on the MCP image of the "zero point" from where the counts created by oxygen atoms were extracted.

Finally, for the response of MCP to neutrals, we assumed that the response of MCP to protons and neutral hydrogen is the same, and that the response to O^+ and O^- is the same as for O. With this assumption, we converted the total hydrogen number (on CR-39) into equivalent count number (using response of MCP to protons as 3 counts/particle) and similarly for O (using response of MCP to O^+ as 12 counts/particle) and added all these equivalent counts for both H and O. It is worth noting that, as anticipated, the ratio of total integrated counts on MCP to the total equivalent counts on CR-39 comes very close to one (i.e., 0.945, within 5%), meaning that the assumption that the response to neutrals (H and O) is the same to the response to protons and O^+ is justified. This is consistent with prior observations, as in Ref. 20, where it was observed that the neutral and ionised charged particle produces the same secondary electron. However, we must note that the discrepancy could be more as we do not know the exact cutoff for hydrogen on CR-39, although we could recognise proton tracks very well down to 40 keV. Another source of error could be the calculation of the particle number below 79 keV on CR-39 by the ratio α. This implies an implicit assumption of similar cross-section for the reaction $O \rightarrow O^-$, over all the energy range, which has to be still investigated.

SUMMARY AND ESSENTIAL NOTE

We have performed the calibration of MCP response to particles with different charge, namely, positive, negative, and neutral. The MCP response to protons (in energy range 0.170–1 MeV), O^+ and O^{2+} (in energy range 0.4–2 MeV), O^- and neutral hydrogen and oxygen atoms were evaluated. It was found that over the measured energy range the response of MCP does not depend on the charge, but it depends on the type of the species, e.g., light (proton) or heavy ions (in this case oxygen).

These calibrations supplement previous calibrations[17] (see Fig. 6), extending the calibrated range of MCP response to protons to lower energies: 0.16–0.5 MeV. Over this range, there is a slow increase of MCP sensitivity for increasing proton energy. In the case of oxygen, one can connect the results to prior results for C^{6+}[17] by assuming that carbon and oxygen ions give similar response on MCP, as indeed the overlap of the data for C^{6+} and O^+ data at 2–3 MeV seems to suggest (see Fig. 6(b)).

ACKNOWLEDGMENTS

This research was supported by Laser Lab Europe proposal MBI001668, EPSRC projects EP/E035728/1-(LIBRA consortium), and EP/E048668/1, projects ELI-Beamlines (Grant No. CZ.1.05/1.1.00 /483 /02.0061), OPVK 3 (Grant No. CZ.1.07/2.3.00/20.0279), and Transregio18 (DFG). R.P. and S.T.-A. thank D. Doria for providing program in MATLAB, P.V.N. acknowledges the support of the World Class University program grant (Grant No. R31-2008-000-10026-0) provided by National Research Foundation (NRF) of Korea.

[1]R. A. Snavely, M. H. Key, S. P. Hatchett, T. E. Cowan, M. Roth, T. W. Phillips, M. A. Stoyer, E. A. Henry, T. C. Sangster, M. S. Singh, S. C. Wilks, A. MacKinnon, A. Offenberger, D. M. Pennington, K. Yasuike, A. B. Langdon, B. F. Lasinski, J. Johnson, M. D. Perry, and E. M. Campbell, Phys. Rev. Lett. **85**, 2945 (2000).

[2]T. E. Cowan, T. E. Cowan, J. Fuchs, H. Ruhl, A. Kemp, P. Audeber, M. Roth, R. Stephens, I. Barton, A. Blazevic, E. Brambrink, J. Cobble, J. Fernández, J.-C. Gauthier, M. Geissel, M. Hegelich, J. Kaae, S. Karsch, G. P. Le Sage, S. Letzring, M. Manclossi, S. Meyroneinc, A. Newkirk, H. Pépin, and N. Renard-LeGalloudec, Phys. Rev. Lett. **92**, 204801 (2004).

[3]M. Hegelich, S. Karsch, G. Pretzler, D. Habs, K. Witte, W. Guenther, M. Allen, A. Blazevic, J. Fuchs, J. C. Gauthier, M. Geissel, P. Audebert, T. Cowan, and M. Roth, Phys. Rev. Lett. **89**, 085002 (2002).

[4]J. Schreiber, F. Bell, F. Gru¨ner, U. Schramm, M. Geissler, M. Schnürer, S. Ter-Avetisyan, B. M. Hegelich, J. Cobble, E. Brambrink, J. Fuchs, P. Audebert, and D. Habs, Phys. Rev. Lett. **97**, 045005 (2006).

[5]V. Malka, J. Faure, Y. A. Gauduel, E. Lefebvre, A. Rousse, and K. T. Phuoc, Nat. Phys. **4**, 447 (2008).

[6]S. Ter-Avetisyan, B. Ramakrishna, M. Borghesi, D. Doria, M. Zepf, G. Sarri, L. Ehrentraut, A. Andreev, P. V. Nickles, S. Steinke, W. Sandner, M. Schnürer, and V. Tikhonchuk, Appl. Phys. Lett. **99**, 051501 (2011).

[7]J. Ishikawa, H. Tsuji, M. Mimura, S. Ikemura, and Y. Gotoh, Surf. Coat. Technol. **103–104**, 173 (1998).

[8]J. Ishikawa *et al.*, Nucl. Instrum. Methods Phys. Res. B **237**, 422–427 (2005).

[9]H. Klein *et al.*, The ESS Technical Study, ESS-96-53-M, November 1996.

[10]B. R. Appleton, J. B. Ball, and J. R. Alonso, "The National spallation neutron source," in *European Particle Accelerator Conference (EPAC'96), Sitges, June 1996*, p. 575.

[11]Y. Takeiri, O. Kaneko, K. Tsumori, Y. Oka, K. Ikeda, M. Osakabe, K. Nagaoka, E. Asano, T. Kondo, M. Sato, and M. Shibuya, Nucl. Fusion **46**, S199–S210 (2006).

[12]Y. Ikeda *et al.*, Nucl. Fusion **46**, S211 (2006).

[13]F. H. Seguin, J. A. Frenje, C. K. Li, D. G. Hicks, S. Kurebayashi, J. R. Rygg, B.-E. Schwartz, R. D. Petrasso, S. Roberts, J. M. Soures, D. D. Meyerhofer, T. C. Sangster, J. P. Knauer, C. Sorce, V. Yu. Glebov, C. Stoeckl, T. W. Phillips, R. J. Leeper, K. Fletcher, and S. Padalino, Rev. Sci. Instrum. **74**, 975 (2003).

[14]D. S. Hey, M. H. Key, A. J. Mackinnon, A. G. MacPhee, P. K. Patel, R. R. Freeman, L. D. Van Woerkom, and C. M. Castaneda, Rev. Sci. Instrum. **79**, 053501 (2008).

[15]A. Mančić, J. Fuchs, P. Antici, S. A. Gaillard, and P. Audebert, Rev. Sci. Instrum. **79**, 073301 (2008); H. Chen, N. L. Back, T. Bartal, F. N. Beg, D. C. Eder, A. J. Link, A. G. MacPhee, Y. Ping, P. M. Song, A. Throop, and L. Van Woerkom, *ibid.* **79**, 033301 (2008).

[16]J. J. Thomson, Philos. Mag. **21**, 225 (1911).

[17]R. Prasad, D. Doria, S. Ter-Avetisyan, P. S. Foster, K. E. Quinn, L. Romagnani, C. M. Brenner, J. S. Green, P. Gallegos, M. J. V. Streeter, D. C. Carroll, O. Tresca, N. Dover, C. A. J. Palmer, J. Schreiber, D. Neely, Z. Najmudin, P. McKenna, M. Zepf, and M. Borghesi, Nucl. Instrum. Methods Phys. Res. A **623**, 712 (2010).

[18]S. Ter-Avetisyan, B. Ramakrishna, R. Prasad, M. Borghesi, P. V. Nickles, S. Steinke, M. Schnürer, K. I. Popov, L. Ramunno, N. V. Zmitrenko, and V. Yu. Bychenkov, Phys. Plasmas **19**, 073112 (2012).

[19]S. Ter-Avetisyan, B. Ramakrishna, D. Doria, G. Sarri, M. Zepf, M. Borghesi, L. Ehrentraut, H. Stiel, S. Steinke, G. Priebe, M. Schnürer, P. V. Nickles, and W. Sandner, Rev. Sci. Instrum. **80**, 103302 (2009).

[20]J. S. Allen, Phys. Rev. **55**, 966 (1939).